fundamental notion that molecular structure, or connectedness, plays an important role in physicochemical and, hence, biological properties. The relation of the connectivity index to other constitutive, additive properties is being pursued.

REFERENCES

(1) L. B. Kier, L. H. Hall, W. J. Murray, and M. Randić, *J. Pharm. Sci.*, **64**, 1971(1975).

(2) L. H. Hall, L. B. Kier, and W. J. Murray, *ibid.*, **64**, 1974(1975).

(3) C. Hansch, J. E. Quinlan, and G. L. Lawrence, *J. Org. Chem.*, **33**, 347(1968).

(4) C. Hansch, in "Medicinal Chemistry," vol. I, E. J. Ariens, Ed., Academic, New York, N.Y.

(5) G. G. Nys and R. F. Rekker, *Chim. Ther.*, **5**, 521(1973).

(6) M. Randić, *J. Amer. Chem. Soc.*, in press.

(7) A. Leo, C. Hansch, and D. Elkins, *Chem. Rev.*, **71**, 525(1971).

(8) M. Tute, *Advan. Drug Res.*, **6**, 1(1971).

(9) C. Hansch and W. J. Dunn, III, *J. Pharm. Sci.*, **61**, 1(1972).

(10) D. J. Crisp and D. H. A. Marr, *Proc. Int. Congr. Surface Activity, 2nd*, **1957**, 310.

(11) H. M. Vernon, *J. Physiol.*, **47**, 15(1913).

(12) E. Kuffer and C. Hansch, *J. Med. Chem.*, **12**, 647(1969).

ACKNOWLEDGMENTS AND ADDRESSES

Received February 10, 1975, from the *Massachusetts College of Pharmacy, Boston, MA 02115*

Accepted for publication April 2, 1975.

The authors acknowledge the assistance of the Eastern Nazarene College Computer Center. L. H. Hall is grateful for the support of Eastern Nazarene College during his sabbatical leave.

* On sabbatical leave from the Department of Chemistry, Eastern Nazarene College, Quincy, MA 02170

[x] To whom inquiries should be directed.

Size Distribution Effects in Multiparticulate Dissolution

PETER VENG PEDERSEN [x] and K. F. BROWN

Abstract □ The evaluation of models for single-particle dissolution, based on multiparticulate dissolution data, is complicated by the distribution effect present when the particles are not truly monodispersed. By using simulated data, it is shown that remarkably good linearity can be obtained with log-normal powders using an incorrect model. It is suggested that particle-size analysis is necessary to enable calculation of the distribution effect and to prevent this type of misinterpretation. The change in particle-size distribution during dissolution is calculated and shows potential for distinguishing between two, but not all three, of the models investigated. Four theoretical rules for multiparticulate dissolution are stated and discussed. The concept of "time scaling" is presented. By using this procedure, it should be possible to reduce considerably computational errors arising from nonlinear dissolution data. It is demonstrated that dissolution profiles can be transformed to a standard form, enabling the distribution effect to be evaluated without interference from rate or particle-size parameters.

Keyphrases □ Dissolution, multiparticulate—size distribution effects, log-normal powders, three single-particle models investigated □ Powders, dissolution—size distribution effects, log-normal distribution profile, three single-particle models investigated □ Particle dissolution—size distribution effects, log-normal powders, three single-particle models investigated

The dissolution profile of a powder is determined by its particle-size distribution and the way the single particles dissolve. Several mathematical models have been presented to describe single-particle dissolution (1–4), but none of these has yet received complete acceptance. Experimental evaluation of the models on the basis of multiparticulate dissolution data is complicated by the distribution effect present when the powder is not truly monodispersed. Such powders are impossible to obtain in most cases (5). Processes such as sieving, precipitation, and grinding do not yield completely uniform particles. This situation is particularly true for fine powders which are of greatest pharmaceutical importance.

In recent years, there has been increasing interest in evaluating the distribution effect in multiparticulate dissolution (6–9). A previous paper (9) discussed the theory and mathematics of multiparticulate systems in relation to single-particle dissolution and the initial size distribution. The present paper evaluates distribution effects for log-normal powder systems; three single-particle dissolution models from the literature are considered. By using simulated dissolution data and particle-size distributions, the possibility of distinguishing between the models is investigated.

THEORY

Let:

$$w = g(w_0,t) \qquad \text{(Eq. 1)}$$

and:

$$w_0 = g^{-1}(w,t) \qquad \text{(Eq. 2)}$$

describe the dissolution equation and inverse dissolution equation, respectively, for a single particle, where w and w_0 are the particle weights at time t and 0, respectively. Further, let $l_0(a_0)$ denote the initial ($t = 0$) particle-size density ("probability") distribution. By assuming that particles are spherical and remain so during dissolution, the particle weight, w, is related to the diameter, a, at any time by $w = \rho\pi a^3/6$, where ρ is the particle density.

By using a technique similar to the one used in a previous paper (9), the following equation can be derived which rigorously describes the particle-size distribution, $l(a)$, at any time if the initial distribution, $l_0(a_0)$, is known together with the particle dissolution function, g:

$$l(a) = \frac{l_0\left(\left[\frac{6}{\pi\rho}g^{-1}\left(\frac{\pi\rho}{6}a^3,t\right)\right]^{1/3}\right)\frac{d}{da}\left[\frac{6}{\pi\rho}g^{-1}\left(\frac{\pi\rho}{6}a^3,t\right)\right]^{1/3}}{\int_{L_1}^{L_2} l_0(a)\,da} \quad \text{(Eq. 3)}$$

for:

$$P\left[\frac{6}{\pi\rho}g\left(\frac{\pi\rho}{6}d_0^3,t\right)\right]^{1/3} \leq a \leq P\left[\frac{6}{\pi\rho}g\left(\frac{\pi\rho}{6}D_0^3,t\right)\right]^{1/3}$$

and $l(a) = 0$ elsewhere.

The integration limits L_1 and L_2 depend on time as follows:

$$L_1 = d_0 \quad \text{for } t \text{ such that } Pg\left(\frac{\pi\rho}{6}d_0^3,t\right) > 0 \quad \text{(Eq. 4a)}$$

$$L_1 = \left[\frac{6}{\pi\rho}g^{-1}(0,t)\right]^{1/3} \quad \text{for } t \text{ such that } Pg\left(\frac{\pi\rho}{6}d_0^3,t\right) = 0 \quad \text{(Eq. 4b)}$$

$$L_2 = D_0 \quad \text{for } t \text{ such that } Pg\left(\frac{\pi\rho}{6}D_0^3,t\right) > 0 \quad \text{(Eq. 4c)}$$

$$L_2 = \left[\frac{6}{\pi\rho}g^{-1}(0,t)\right]^{1/3} \quad \text{for } t \text{ such that } Pg\left(\frac{\pi\rho}{6}D_0^3,t\right) = 0 \quad \text{(Eq. 4d)}$$

where d_0 and D_0 denote the initial diameters of the smallest and largest particles, respectively. The operator P has been introduced to make the expression generally applicable (9). It is defined to be equal to one in the time period before the operand becomes zero and is equal to zero beyond that time. The lower integration limit, L_1, changes value at $g[(\rho\pi/6)d_0^3,t] = 0$, that is the critical time, when the particles start to disappear. The time at which $g[(\rho\pi/6)D_0^3,t] = 0$ corresponds to the disappearance of the last particle and marks the completion of the dissolution process.

Many powders have size distributions that are approximately log-normal (5). Consider such a powder distributed such that $\ln a_0$ approximates a normal distribution with mean μ and standard deviation σ truncated at $\ln d_0 = \mu - i\sigma$ and $\ln D_0 = \mu + j\sigma$, where i and j are truncation parameters. The initial particle-size distribution, $l_0(a_0)$, is then given by (9):

$$l_0(a_0) = \frac{a_0^{-1}N(\ln a_0,\mu,\sigma)}{\int_{d_0}^{D_0} a_0^{-1}N(\ln a_0,\mu,\sigma)da_0} \qquad d_0 \leq a_0 \leq D_0 \quad \text{(Eq. 5)}$$

where $N(\,)$ is the normal distribution with $\ln a_0$ as the variable.

The change in the particle-size distribution during dissolution depends on the way the individual particles dissolve. Three widely known models for single-particle dissolution are considered. When written in the same form as Eq. 1, the Hixson–Crowell "cube root law" (3) can be expressed as:

$$w = (w_0^{1/3} - k_3t)^3 \quad \text{(Eq. 6)}$$

In a similar way, the equation presented by Niebergall *et al.* (2) can be written simply:

$$w = (w_0^{1/2} - k_2t)^2 \quad \text{(Eq. 7)}$$

and the model proposed by Higuchi and Hiestand (1) can be written:

$$w = (w_0^{2/3} - k_1t)^{3/2} \quad \text{(Eq. 8)}$$

For simplicity and because their evaluation is not important to the theoretical discussion, the constants k_1, k_2, and k_3 are used in place of the original time coefficients which included parameters such as the shape factor, particle density, and diffusion coefficient. In the following discussion, Eqs. 8, 7, and 6 will be referred to as Models 1, 2, and 3, respectively.

By having defined the initial size distribution, $l_0(a_0)$ (Eq. 5), and the dissolution function (Eqs. 6–8), the size distribution at time t, $l(a)$, can be expressed applying Eq. 3:

$$l(a) = \frac{a^{\left(\frac{3}{m}-1\right)}(a^{\frac{3}{m}} + Kt)^{-1}N[\ln(a^{\frac{3}{m}} + Kt)^{\frac{m}{3}},\mu,\sigma]}{F\left(\frac{T_2-\mu}{\sigma}\right) - F\left(\frac{T_1-\mu}{\sigma}\right)} \quad \text{(Eq. 9)}$$

for:

$$P(e^{\frac{3}{m}(\mu-i\sigma)} - Kt)^{\frac{m}{3}} \leq a \leq P(e^{\frac{3}{m}(\mu+j\sigma)} - Kt)^{\frac{m}{3}}$$

and $l(a) = 0$ elsewhere. Also:

$$T_1 = \mu - i\sigma \quad \text{for } \frac{m}{3}\ln(Kt) < \mu - i\sigma \quad \text{(Eq. 10a)}$$

$$T_1 = \frac{m}{3}\ln(Kt) \quad \text{for } \frac{m}{3}\ln(Kt) \geq \mu - i\sigma \quad \text{(Eq. 10b)}$$

$$T_2 = \mu + j\sigma \quad \text{for } \frac{m}{3}\ln(Kt) < \mu + j\sigma \quad \text{(Eq. 10c)}$$

$$T_2 = \frac{m}{3}\ln(Kt) \quad \text{for } \frac{m}{3}\ln(Kt) \geq \mu + j\sigma \quad \text{(Eq. 10d)}$$

and:

$$K = (6/\rho\pi)^{\frac{1}{m}}k \quad \text{(Eq. 11)}$$

Equation 9 describes the size distribution for all three models. For Model 1, $m = 3/2$; for Model 2, $m = 2$; and for Model 3, $m = 3$. The constants k and K for each model should be k_1, k_2, and k_3 and K_1, K_2, and K_3, respectively. The function $F(\,)$, the commonly tabulated area under the standard normal curve function, is defined as:

$$F(x) = \int_{-\infty}^{x}(1/\sqrt{2\pi})e^{-\frac{x^2}{2}}\,dx \quad \text{(Eq. 12)}$$

The mean particle size (diameter), $\bar{a}$, can be obtained by applying the usual integration approach used in mathematical expectation:

$$\bar{a} = \frac{\int_R a^{\frac{3}{m}}(a^{\frac{3}{m}} + Kt)^{-1}N[\ln(a^{\frac{3}{m}} + Kt)^{\frac{m}{3}},\mu,\sigma]da}{F\left(\frac{T_2-\mu}{\sigma}\right) - F\left(\frac{T_1-\mu}{\sigma}\right)} \quad \text{(Eq. 13)}$$

The integration interval R in Eq. 13 is the same as the interval for a defined in Eq. 9. Equation 13 considers Models 1 and 2 ($m = 3/2$ and $m = 2$, respectively). The mean particle size for the third model ($m = 3$) simplifies further to:

$$\bar{a} = \frac{F\left(\frac{T_2-\mu}{\sigma} - \sigma\right) - F\left(\frac{T_1-\mu}{\sigma} - \sigma\right)}{F\left(\frac{T_2-\mu}{\sigma}\right) - F\left(\frac{T_1-\mu}{\sigma}\right)}e^{\mu+\sigma^2/2} - K_3t \quad \text{(Eq. 14)}$$

where T_1 and T_2 are still defined as in Eqs. 10a–10d. The exact dissolution profile of a log-normal powder with single particles dissolving according to each of the three models can be derived using Eq. 13 presented in the previous paper (9):

$$\frac{W}{W_0} = \sum_{n=0}^{m}\binom{m}{n}(-Kt)^{(m-n)} \times \frac{F\left(\frac{T_2-\mu}{\sigma} - \frac{3n\sigma}{m}\right) - F\left(\frac{T_1-\mu}{\sigma} - \frac{3n\sigma}{m}\right)}{F(j-3\sigma) - F(-i-3\sigma)} \times e^{\frac{3}{m}(n-m)[\mu+\frac{3}{m}(n+m)\sigma^2/2]} \quad \text{(Eq. 15)}$$

where W_t and W_0 are the amounts of undissolved powder at time t and 0, respectively. Equation 15 with $m = 3$, although presented in more compact form, is identical to Eq. 18 in the previous paper (9). Equation 15 is not defined for Model 1 ($m = 3/2$), which must be considered separately:

$$\frac{W}{W_0} = \frac{\int_{R_1}^{R_2}(w^2 - K_1t)^{3/2}w^{-1}N(\ln w,\mu,\sigma)\,dw}{F(j-3\sigma) - F(-i-3\sigma)}e^{-3\mu-9\sigma^2/2} \quad \text{(Eq. 16)}$$

where:

$$R_1 = e^{\mu-i\sigma} \quad \text{for } (K_1t)^{1/2} < e^{\mu-i\sigma} \quad \text{(Eq. 17a)}$$

$$R_1 = (K_1t)^{1/2} \quad \text{for } (K_1t)^{1/2} \geq e^{\mu-i\sigma} \quad \text{(Eq. 17b)}$$

$$R_2 = e^{\mu+j\sigma} \quad \text{for } (K_1t)^{1/2} < e^{\mu+j\sigma} \quad \text{(Eq. 17c)}$$

$$R_2 = (K_1t)^{1/2} \quad \text{for } (K_1t)^{1/2} \geq e^{\mu+j\sigma} \quad \text{(Eq. 17d)}$$

The derivations of these equations are based on two assumptions: (*a*) that the particles in the multiparticulate system dissolve

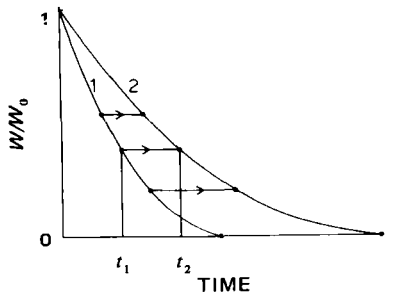

Figure 1—*Two dissolution curves having the same intrinsic dissolution profile. Curve 1 can be brought into curve 2 by a time-scaling factor,* t_2/t_1. *Rule 2 states that* $k_{(1)} = (t_2/t_1)k_{(2)}$, *where* $k_{(1)}$ *and* $k_{(2)}$ *are the rate parameters in the single-particle dissolution equation for Systems 1 and 2 having the same particle-size distribution. These statements also include plots where* W/W_0 *is raised to any other exponent.*

independently of each other, which will be approximated well under sink conditions; and (*b*) that they dissolve according to the same single-particle dissolution model having fixed parameters (for these cases, k_1, k_2, and k_3 are the same for all particles and do not vary during the dissolution). If these conditions exist, then it is possible to make some general rules concerning the dissolution process. These rules are explained in relation to what will be termed "the intrinsic dissolution profile," which can be defined in the following way. Dissolution curves have the same intrinsic dissolution profile if, by a suitable scaling of time, they can be brought into each other in a W/W_0 *versus* time plot (Fig. 1).

It should be clear from observation of Eqs. 12 and 13 in the previous paper (9) that the coefficient of time in an expression correctly defining the multiparticulate dissolution profile originates directly from the coefficient of time in the single-particle dissolution equation. Thus, a different value of the rate parameter, that is, a different coefficient of time in the single-particle dissolution equation, has the same effect as a different scaling of time. Therefore, the intrinsic dissolution profile will still be the same. The following rule can thus be stated:

1. *The intrinsic dissolution profile is independent of the value of the rate parameter, that is, the coefficient of time in the single-particle dissolution equation.*

According to this rule, the rate parameters k_1, k_2, and k_3 (Eqs. 6–8) have no influence on the intrinsic dissolution profile. Furthermore, there will always be a proportional relationship between the coefficient of time in the multiparticulate dissolution equation and the rate parameter [note, for example, that K in Eqs. 15 and 16 is related to k by $K = (6/\rho\pi)^{1/m}k$ as seen in Eq. 11]. The following rule can therefore be stated:

2. *In two systems having identical particle-size distributions, the time-scaling factor that brings one dissolution curve into another is equal to the factor with which the rate parameters are proportionally related in the two systems* (Fig. 1).

Consider two particle-size distributions that on a logarithmic scale are distributed $l_1(\log a)$ and $l_2(\log a)$, having the same shape. Then, for any diameter, a (Fig. 2) $l_1(\log a) = l_2(\log a + \log K_a)$;

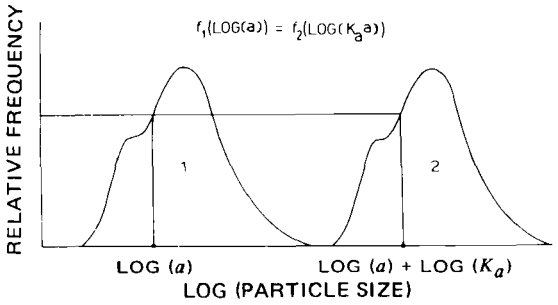

Figure 2—*Two particle-size distributions having the same shape on a logarithmic scale. According to Rule 3, these distributions result in dissolution curves with the same intrinsic dissolution profile (for example, curves 1 and 2 of Fig. 1).*

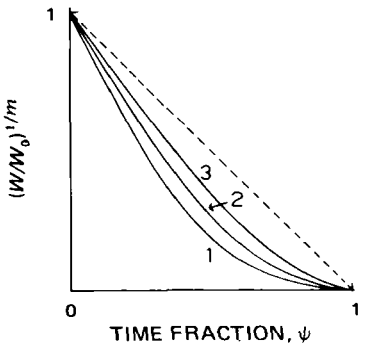

Figure 3—*Normalized dissolution profiles of powders initially log-normal* ($\sigma = 0.2$, i = j = 2), *calculated (Eqs. 16 and 19) to dissolve and plotted according to Models 1, 2, and 3: Model 1,* m = 3/2; *Model 2,* m = 2; *and Model 3,* m = 3. *The stippled line represents monodispersed powders* ($\sigma = 0$).

i.e., $l_1(\log a) = l_2(\log K_a a)$, where $\log K_a$ is a measure of the distance between the logarithmic distributions. Therefore, if the particles in System 2 are scaled (measured) in units of K_a, the resulting distribution is the same as that for System 1. Such a scaling of the particle sizes has an effect on the calculated dissolution profile.

However, if the coefficient of time in the single-particle dissolution equation is dimensionally dependent on length, as in a model that is not first order, then a scaling in length, as in the above transformation of the particle-size distribution, has the same effect as a scaling in time. If the single-particle dissolution is a first-order process, then the dissolution profile is completely independent of the particle-size distribution, because the fraction of each particle that dissolves in a given time is the same, independent of its size. Therefore, it can be concluded that Systems 1 and 2 have the same intrinsic dissolution profile, and the following rule can be given:

3. *Two powders dissolving according to the same single-particle dissolution model have the same intrinsic dissolution profile if their particle-size distributions are of the same shape on a logarithmic scale* (Fig. 2).

It follows from this rule that it is not the "position" of the distribution, that is, not the actual size of the particles, but the shape of the distribution that affects the intrinsic dissolution profile. Thus it can be stated that:

4. *The intrinsic dissolution profile does not depend on the actual sizes of the particles but on the shape of their distribution.*

RESULTS AND DISCUSSION

According to Rule 2, the concept of time scaling in dissolution studies should have some practical application. It already has been stated that it is impossible to prepare completely monodispersed powders; therefore, some nonlinearity always is present in the dissolution profile due to the distribution effect (9). This nonlinearity

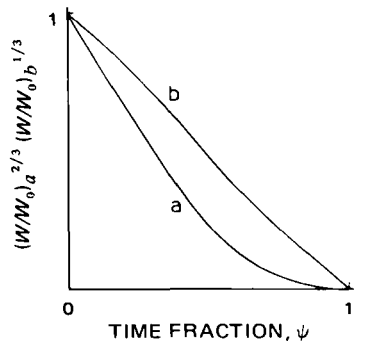

Figure 4—*Normalized dissolution profiles of powders initially log-normal* ($\sigma = 0.14$, i = j = 2), *calculated (Eq. 16) to dissolve and plotted according to Model 1 (curve a). Curve b is the same data plotted according to Model 3, resulting in almost complete cancellation of the size distribution effect observed in curve a.*

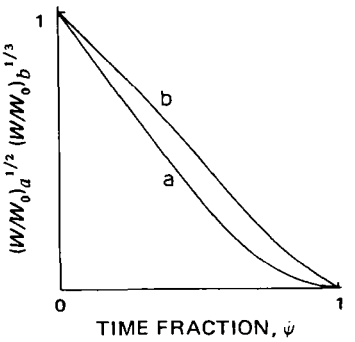

Figure 5—*Normalized dissolution profiles of powders initially log-normal (σ = 0.12, i = j = 2), calculated (Eq. 19, m = 2) to dissolve and plotted according to Model 2 (curve a). Curve b is the same data plotted according to Model 3, resulting in almost complete cancellation of the size distribution effect observed in curve a.*

introduces errors into determination of the influence of factors such as the stirring rate, temperature, and vehicle composition on the rate parameter (k_1, k_2, or k_3) using conventional "initial slope" or "line of best fit" computational techniques.

However, Rule 2 provides an alternative approach where this type of error is negligible. The new technique simply involves finding a time-scaling factor that brings one curve into the other or, more correctly, minimizes the separation of the curves. This factor is then equal to the factor by which the two rate parameters are proportionally related. Possibly the best criterion is to minimize the squared horizontal differences between the curves.

According to Rules 1 and 3, it should be possible to normalize the calculated dissolution profiles for log-normal powders by appropriate scaling of time to a form that does not depend on either the rate parameter (k_1, k_2, or k_3) or the actual sizes of the particles. One approach is to scale the time in the W/W_0 *versus* time plots as the time fraction, ψ, defined as the fraction of the time necessary for complete dissolution. The expression defining the resulting normalized dissolution profile can be obtained in the following way, using Models 2 and 3 as examples. The time for complete dissolution, t_0, is given by $(m/3)\ \ln\ (Kt_0) = \mu + j\sigma$ (Eqs. 9 and 15); then since $\psi = t/t_0$, it follows that:

$$\psi = Ke^{-\frac{3}{m}(\mu + j\sigma)}t \qquad \text{(Eq. 18)}$$

Accordingly, the Kt terms in Eq. 15 can be substituted by

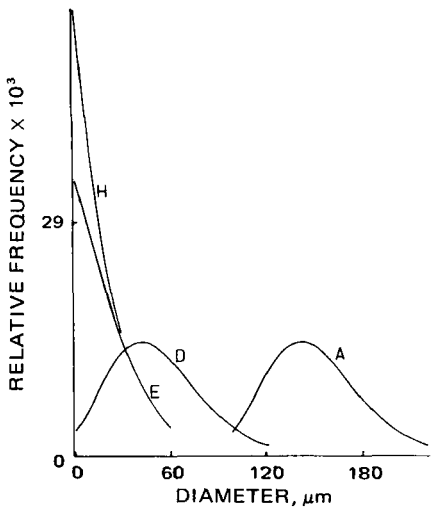

Figure 6—*Size distribution change with time for a powder initially log-normal (μ = 5, σ = 0.2, i = j = 2), calculated (Eq. 9, m = 3) to dissolve according to Model 3. Distributions are labeled in chronological order. Key: A, initial distribution; and D, distribution at critical time.*

$\psi^{3(\mu+j\sigma)/m}$, which causes the μ terms to cancel out. After rearrangement, Eq. 15 can be written:

$$\frac{W}{W_0} = \sum_{n=0}^{m}\binom{m}{n}(-\psi)^{(m-n)}\frac{F\left(j - \frac{3n\sigma}{m}\right) - F(A)}{F(j - 3\sigma) - F(-i - 3\sigma)} \times e^{\frac{3}{m}(n-m)(-j\sigma + \frac{3}{m}(n+m)\sigma^2/2)} \qquad \text{(Eq. 19)}$$

where:

$$A = i - \frac{3n\sigma}{m} \qquad \text{for } 0 \le \psi < e^{-\frac{3}{m}(i+j)m} \qquad \text{(Eq. 20)}$$

and:

$$A = j + \frac{m \ln \psi}{3\sigma} - \frac{3n\sigma}{m} \qquad \text{for } e^{-\frac{3}{m}(i+j)m} \le \psi \le 1 \qquad \text{(Eq. 21)}$$

It is seen that the normalized dissolution profile (Eq. 19, m = 2 or m = 3) does not contain any rate terms (k_3 or k_2 from Eq. 6 or 7) or any term (μ) representing the sizes of the particles[1]. Scaling of time according to Eq. 18 has brought all dissolution curves originating from distributions with the same "logarithmic shape" (which is completely defined by parameters σ, i, and j) into one single curve (Eq. 19) which does not depend on the sizes of the particles or the rate parameter from the single-particle equation. This finding confirms Rules 1 and 3.

The transformation has essentially normalized all possible systems having the same intrinsic dissolution profile into one single curve. This curve is unique in that it makes it possible to evaluate the isolated distribution effect. This evaluation is best done by plotting in a way that linearizes the underlying single-particle dissolution equation (Eqs. 6–8), by using $(W/W_0)^{1/m}$ instead of W/W_0 in the plot. Such a plot will be linear with slope = −1 for a true monodispersed system. Any deviation from this linearity and slope will be due solely to the distribution effect.

Figure 3 shows such normalized dissolution profiles, calculated according to Eqs. 16 and 19, for powders initially log-normal, having distribution (shape) parameters σ = 0.2 and $i = j = 2$, for particles dissolving according to each of the three models[2] (Eqs. 6–8). The fraction of undissolved powder, W/W_0, is raised to the powers of 1/3, 1/2, and 2/3 for the reason just given. The distribution effect is smallest for Model 3 and greatest for Model 1. Remarkably good linearity is observed for the first part of the dissolution process for all three models. This result does not mean, however, that the distribution effect is negligible in the beginning, as is seen from the fact that the slopes differ considerably from −1.

It is obvious that good linearity in such plots is no necessary guarantee that the powder is monodispersed or that there is no distribution effect. This error has been made frequently in investigations where the dissolution process is not followed to the end or very near the end. Furthermore, the validity of a particular dissolution model cannot always be assessed solely from the linearity of a plot of data according to that model *even when the dissolution is followed to the very end.* This fact is clearly demonstrated in Figs. 4 and 5.

Curve a in Fig. 4 shows a normalized dissolution profile of log-normal powders (σ = 0.14, $i = j = 2$) calculated (Eq. 16) to dissolve and plotted (W/W_0 to power of 2/3) according to Model 1. The size distribution effect is clearly reflected in the nonlinearity of the curve. By plotting the same data according to an incorrect model, Model 3 (W/W_0 to power of 1/3), the size distribution effect is almost entirely canceled and surprisingly good linearity is obtained *that extends to the very end of the dissolution process* (curve b). Figure 5 shows the same phenomenon for powders (σ = 0.12, $i = j$ = 2) where the particles are calculated to dissolve according to Model 2 (Eq. 19, m = 2).

A judgment based solely on the linearity of such plots will often

[1] The normalized dissolution profile can also be obtained directly from Eq. 15 or 16 by choosing an arbitrary value for μ and calculating W/W_0 for different Kt values, ranging from 0 to $e^{3(\mu+j\sigma)/m}$, corresponding to a set of ψ values (Eq. 18). This technique was applied for Model 1 using Eq. 16. The computations were done for a wide range of μ values and showed independence of this parameter, in agreement with theory.

[2] A CDC Cyber 76 digital computer, equipped with calcomp plotter, was used for calculations and plots. Numerical evaluations were tested to six digits.

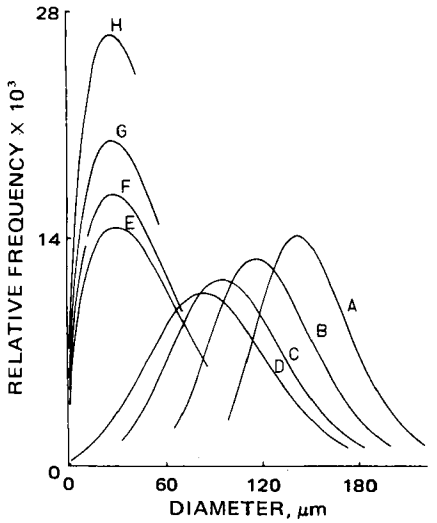

Figure 7—*Size distribution change with time for a powder initially log-normal ($\mu = 5$, $\sigma = 0.2$, i = j = 2), calculated (Eq. 9, m = 2) to dissolve according to Model 2. Distributions are labeled in chronological order. Key: A, initial distribution; and D, distribution at critical time.*

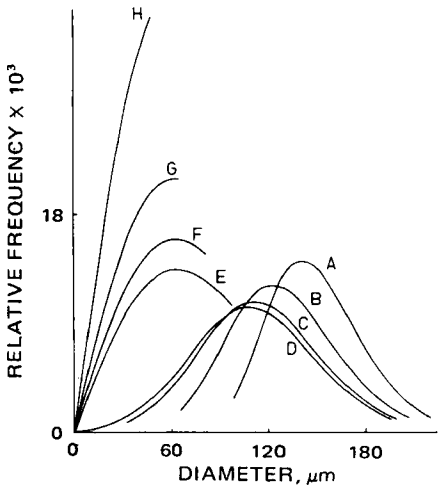

Figure 8—*Size distribution change with time for a powder initially log-normal ($\mu = 5$, $\sigma = 0.2$, i = j = 2), calculated (Eq. 9, m = 3/2) to dissolve according to Model 1. Distributions are labeled in chronological order. Key: A, initial distribution; and D, distribution at critical time.*

lead to false conclusions about the validity of the model, even where dissolution is followed to completion, unless an analysis of particle size is made. The phenomena demonstrated in Figs. 4 and 5 are not special cases for the particular values of σ chosen but were observed to apply for a wide range of σ values.

These findings clearly emphasize the importance of particle-size analysis in investigations of dissolution kinetics. It is of interest to see how the particle-size distribution changes during dissolution. The distribution of a powder that is initially log-normal ($\mu = 5$, $\sigma = 0.2$, $i = j = 2$) was calculated at various times according to Eq. 9 and plotted in Figs. 6, 7, and 8, illustrating dissolution according to Models 3, 2, and 1, respectively. The distributions are labeled in chronological order from A to H. Curves A and D represent the distributions initially and at critical time, respectively.

When particles dissolve according to Model 3 (Fig. 6), then the shape of the size distribution remains constant before critical time, consistent with isotropic dissolution ($da/dt = -K_3$). This is not the case for dissolution according to Models 1 and 2 where the absolute rate of change in size of the particles, da/dt, increases with time. For Model 1:

$$da/dt = -\frac{K_1}{2}(a_0^2 - K_1 t)^{-1/2} \qquad \text{(Eq. 22)}$$

and for Model 2:

$$da/dt = -\frac{2}{3}K_2(a^{3/2} - K_2 t)^{-1/3} \qquad \text{(Eq. 23)}$$

As a result, the distribution broadens before critical time (Figs. 7 and 8) and is particularly affected at the small particle end as zero is approached where da/dt takes extreme values. Because of the latter effect, near the end of the dissolution process the relative frequency of the very small particles increases with increasing size for Models 1 and 2 (Figs. 8 and 7) while it decreases for Model 3 (Fig. 6). This information should be of value for distinguishing Model 3 from the two others. However, from the distribution change alone, it is difficult to distinguish between Models 2 and 3.

It appears from this discussion that it is not possible to distinguish clearly between all three models from dissolution data or from particle-size measurements alone. It would be of interest to determine whether this could be done if both types of information are combined quantitatively. One convenient combination seems to have potential for discriminating between the models. It will be called the dispersion product, s, and is defined as:

$$s = \left(\frac{\bar{a}}{\bar{a}_0}\right)^3 \times \frac{W_0}{W} \qquad \text{(Eq. 24)}$$

where $\bar{a}$ and $\bar{a}_0$ are the mean particle diameters at times t and 0, respectively. The dispersion product is readily obtained, requiring only information for the fraction dissolved and simple averages from particle-size measurements. Time-consuming evaluations of distribution parameters are not required. It is a dimensionless variable that depends only on the initial distribution parameter, σ (for fixed i and j), and the single-particle dissolution equation[3]. The variation of s during the dissolution period should for this reason reflect the basic equation.

Figure 9 shows this variation for powders initially log-normally distributed ($\sigma = 0.2$, $i = j = 2$). The curves representing the three dissolution models are significantly different. The basic shape of the curves remains the same for varying values of σ, although the minima shift to the right and to higher values for very narrow distributions. All three curves approach $s = 1$ (stippled line) when σ approaches zero as expected for a completely monodispersed powder. The values of the three minima remain approximately con-

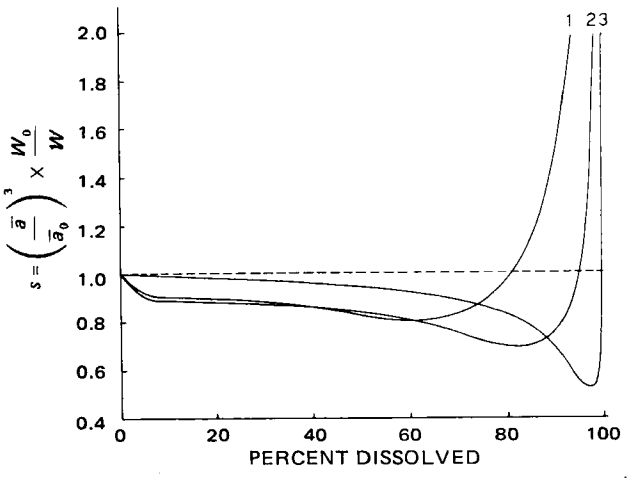

Figure 9—*Variation of the dispersion product (Eq. 24), with progress of dissolution of powders initially log-normal ($\sigma = 0.2$, i = j = 2), calculated (Eqs. 13, 14, 16, and 19) to dissolve according to Models 1, 2, and 3. The stippled line represents a monodispersed powder ($\sigma = 0$).*

[3] The numerical evaluation of the dispersion product was made using several widely different arbitrarily chosen values for μ and confirmed that this parameter cancels out in the calculations as expected. It is clear from previous discussions that s does not depend on the value of the rate parameter (k_1, k_2, or k_3 in Eqs. 6–8).

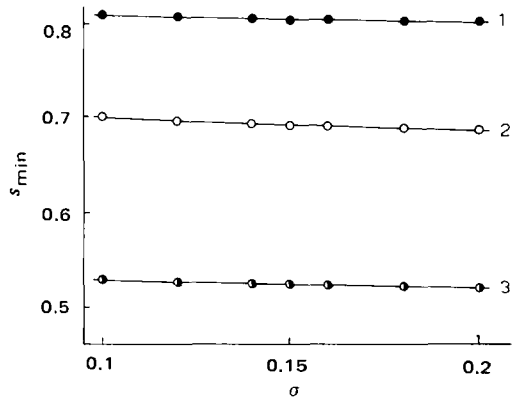

Figure 10—*Variation of dispersion product minima, s_{min}, with the initial distribution parameter, σ, for dissolution according to Models 1, 2, and 3* (i = j = 2).

stant when σ ranges from somewhat less than 0.1 to at least 0.2 (Fig. 10), which should encompass most fine powder distributions encountered in practice. Theoretically, the considerable difference between the s_{min} values should make it possible to distinguish clearly between the three models.

The dispersion product profile (s *versus* W/W_0 or percent dissolved) has some powerful properties, since it is a dimensionless quantity dependent only on the *shape* of the distribution and the *form* of the single-particle dissolution equation. Any change in the coefficient of time k_1, k_2, or k_3 (Eqs. 6–8) during the dissolution will have no effect on the s profile, because s is essentially parametrically represented by the time, provided the change is the same for all particles irrespective of their size. Thus, if changes in such conditions as temperature, agitation, or vehicle composition during dissolution have identical influence on all particles, these changes will have no effect on the s profile. Alternatively, if the external conditions are maintained constant, then s should indicate whether the coefficients are independent of particle size and, hence, whether such parameters as the interfacial concentration gradient, shape factor, and interfacial reaction rate are independent of particle size. The dispersion product should, therefore, be a valuable tool in dissolution kinetic studies.

The extent to which these mathematical models can be applied to describe the dissolution of a "real" powder depends on three assumptions.

1. As mentioned earlier, it was assumed that the particles dissolve independently of each other. This should be approximated well under sink conditions.

2. It was assumed that the dissolution of each particle in the powder can be described by an equation having the same parameter value (k) for all of the particles. In practice, this assumption is rarely valid because of differences in individual particle shapes, crystal structure, and interaction with the vehicle. However, these types of effects probably can be averaged to produce a parameter value for the single-particle dissolution model which, when used in the multiparticulate dissolution equation, results in a good approximation of the actual multiparticulate dissolution behavior.

3. It was assumed that the initial particle-size distribution can be approximated by a truncated log-normal distribution. Although it is generally accepted that most powders are approximately "log-normal," it is likely that the log-normal distribution function only provides a coarse approximation of the actual particle-size distribution, which usually contains a number of irregularities.

This paper has dealt only with log-normal powders and three dissolution models. However, Eq. 3, together with Eq. 13 from the previous paper (9), makes it possible to calculate dissolution characteristics for a powder of any initial size distribution, or a sieve fraction of such a powder, considering any single-particle dissolution equation of explicit form.

SYMBOLS

w = weight of dissolving particle at time t
w_0 = initial weight of particle
$W = \sum w$ = weight of undissolved powder at time t
$W_0 = \sum w_0$ = initial weight of powder
a = diameter of dissolving particle at time t
a_0 = initial diameter of particle
$\bar{a}$ = mean particle diameter at time t
$\bar{a}_0$ = initial mean particle diameter
t = time
$N(x,\mu,\sigma) = (1/\sigma\sqrt{2\pi})e^{(x-\mu)^2/2\sigma^2}$ = normal distribution function
μ = mean of normal distribution
σ = standard deviation of normal distribution
i, j = lower and upper truncation parameters for the initial size distribution that is log-normal and truncated at $\ln a_0 = \mu - i\sigma$ and $\ln a_0 = \mu + j\sigma$
d_0 = min a_0 ($\ln d_0 = \mu - i\sigma$)
D_0 = max a_0 ($\ln D_0 = \mu + j\sigma$)
$F(x) = \int_{-\infty}^{x} (1/\sqrt{2\pi})e^{-x^2/2}\,dx$ = area under standard normal distribution function
$w = g(w_0,t)$ = particle dissolution function (for example, Eqs. 6–8)
$w_0 = g^{-1}(w,t)$ = inverse particle dissolution function
$l(a)$ = particle-size density distribution at time t
$l_0(a_0)$ = initial particle-size density distribution
Model 1 = $w = (w_0^{2/3} - k_1 t)^{3/2}$
Model 2 = $w = (w_0^{1/2} - k_2 t)^2$
Model 3 = $w = (w_0^{1/3} - k_3 t)^3$
ψ = time fraction = fraction of time necessary for complete dissolution
m = 3/2, 2, and 3 for Models 1, 2, and 3, respectively
k_i = parameter in model, i = 1–3
$K_i = (6/\rho\pi)^{1/m} k_i$
$s = (\bar{a}/\bar{a}_0)^3 \times W_0/W$, dispersion product
$\binom{m}{n} = m!/[n!\,(m-n)!]$, binomial coefficient
P = operator that is equal to 1 in the time period before the operand becomes equal to zero and is equal to zero after that time

REFERENCES

(1) W. I. Higuchi and E. N. Hiestand, *J. Pharm. Sci.*, **52,** 67(1963).

(2) P. J. Niebergall, G. Milosovich, and J. E. Goyan, *ibid.*, **52,** 236(1963).

(3) A. W. Hixson and J. H. Crowell, *Ind. Eng. Chem.*, **23,** 923(1931).

(4) J. E. Goyan, *J. Pharm. Sci.*, **54,** 645(1965).

(5) "Symposium on Particle Size Measurement," American Society for Testing Materials Special Technical Publication No. 234, Philadelphia, Pa., 1958.

(6) J. T. Carstensen and M. N. Musa, *J. Pharm. Sci.*, **61,** 223(1972).

(7) D. Brooke, *ibid.*, **62,** 795(1973).

(8) *Ibid.*, **63,** 344(1974).

(9) P. V. Pedersen and K. F. Brown, *J. Pharm. Sci.*, **64,** 1192(1975).

ACKNOWLEDGMENTS AND ADDRESSES

Received October 25, 1974, from the *Department of Pharmacy, University of Sydney, Sydney, N.S.W. 2006, Australia.*

Accepted for publication April 2, 1975.

Supported in part by Grant 72/9184 from the National Health and Medical Research Council of Australia.

[x] To whom inquiries should be directed